ISSN 1063-7826, Semiconductors, 2018, Vol. 52, No. 14, pp. 1791–1794. © Pleiades Publishing, Ltd., 2018.

EXCITONS
IN NANOSTRUCTURES

Classification of Energy States of the Exciton in Square Quantum Well[1]

P. A. Belov

Department of Computational Physics, St. Petersburg State University, St. Petersburg, 198504 Russia
e-mail: pavelbelov@gmail.com

Abstract—The energy states of the exciton in a single square GaAs-based quantum well are obtained from a numerical solution of the three-dimensional Schrödinger equation for the envelope of the exciton wave function. This equation is based on the exciton effective energy operator with a spherical approximation of the Luttinger Hamiltonian. The calculated states are classified based on the types of one-dimensional functions for the factorized form of the wave function. The upper limit for the energies of the exciton states in a quantum well is confirmed by the complex scaling method.

DOI: 10.1134/S1063782618140038

INTRODUCTION

Energy states of excitons in quantum wells (QWs) and their radiative properties have been intensively experimentally studied by methods of photoluminescence and optical reflectance spectroscopy [1–3]. A quality of heterostructures is permanently growing and new experimental data on the energies of exciton resonances and the exciton-light coupling have become available recently [4–6].

A purely theoretical description of exciton states in QWs is difficult due to the degenerate valence band as well as an interplay of the QW potential and the Coulomb electron–hole (e–h) interaction. A reliable solution is numerically obtained only for narrow or very wide QWs ($L < 10$ nm and $L > 150$ nm for the GaAs QWs) [3]. For narrow QWs, it has been mainly calculated by the variational method [7, 8] and was usually restricted to the exciton ground state. Recently, more advanced approach has been developed for narrow QWs [9], however, a complete e–h spectrum for a broad range of QW widths has not been understood thoroughly.

We developed a method for a precise numerical solution of the Schrödinger equation for the exciton in the single square QW of a finite barrier [10–12]. The Schrödinger equation is reduced to the three-dimensional equation, which is solved by the finite-difference method [13]. As a result, we determine energies and wave functions of the s-like exciton states. It also allows us to obtain the radiative decay rates, Γ_0, for calculated states. The computations made it possible to thoroughly study a dependence of the energy levels on the QW width. The upper boundary of the e–h bound states in QW was determined by the complex-scaling method [14–16], that was applied to this problem for the first time. The energy levels of the e–h bound states were classified based on the types of one-dimensional functions for the factorized form of the wave function. In calculations, we modeled the heavy-hole exciton states in a heterostructure with $GaAs/Al_{0.3}Ga_{0.7}As$ QW.

THEORETICAL MODEL

We calculate the exciton states in a single square QW from a solution of the three-dimensional equation derived from the Schrödinger equation for the exciton. For simplicity, a spherical approximation of the Luttinger Hamiltonian [17] is used as well as the light-hole-heavy-hole mixing is ignored. This three-dimensional homogeneous equation for s-like exciton states is given as [10]

$$\left(K - \frac{e^2}{\epsilon\sqrt{\rho^2 + (z_e - z_h)^2}} + V_e(z_e) + V_h(z_h)\right) \times f(z_e, z_h, \rho) = E_X f(z_e, z_h, \rho),$$

where the kinetic term with constant effective masses reads

$$K = -\frac{\hbar^2}{2m_e}\frac{\partial^2}{\partial z_e^2} - \frac{\hbar^2}{2m_{hz}}\frac{\partial^2}{\partial z_h^2} - \frac{\hbar^2}{2\mu}\left(\frac{\partial^2}{\partial \rho^2} - \frac{1}{\rho}\frac{\partial}{\partial \rho} + \frac{1}{\rho^2}\right).$$

In the equations, the unknown function f is related to the three-dimensional wave function φ as [10, 11] $\varphi(z_e, z_h, \rho) = f(z_e, z_h, \rho)/\rho$, where radius in the xy-plane

[1] The article is published in the original.

$\rho = \sqrt{(x_e - x_h)^2 + (y_e - y_h)^2}$. Terms $V_{e,h}(z_{e,h})$ are QW potentials. The symbol μ denotes the reduced effective mass in the xy-plane, m_{hz} is the hole mass in the z-direction. The exciton binding energy, E_b, is defined by the exciton ground state energy, E_X, with respect to the lowest quantum-confinement energies of the electron, E_{e1}, and the hole, E_{h1}, in QW: $E_b = E_{e1} + E_{h1} - E_X$. Energies E_{e1} and E_{h1} are obtained from a solution of one-dimensional Schrödinger equations for the carriers in the QW. The sum $E_{e1} + E_{h1}$ defines the lower boundary of the continuous spectrum, thus gives the upper energy limit for the states of the exciton in QW.

The exciton-light coupling is characterized by the radiative decay rate, Γ_0, which describes a radiative broadening of the exciton resonance. For the exciton in QW, the radiative decay rate is given by expression [3]:

$$\Gamma_0 = \frac{2\pi q}{\hbar\epsilon}\left(\frac{e|p_{cv}|}{m_0\omega_0}\right)^2\left|\int_{-\infty}^{\infty}\varphi(z,z,0)e^{iqz}dz\right|^2.$$

Here, $z = z_e = z_h$, $q = \omega\sqrt{\epsilon}/c$ is the light wave vector, ω_0 is the exciton frequency, m_0 is a mass of the electron in vacuum, ϵ is the dielectric constant, $|p_{cv}|$ is the matrix element of the momentum operator between the single-electron conduction- and valence-band states.

The exponential decrease of the wave functions at large values of variables allows us to impose zero boundary conditions for the function $f(z_e, z_h, \rho)$ at the boundary of some rectangular domain. The obtained boundary value problem for the three-dimensional homogeneous equation was accurately solved. For discretization of the equation we employed the second-order finite-difference approximation [13]. It produces a sparse block-tridiagonal matrix [18]. A small part of the matrix spectrum was obtained by the Arnoldi algorithm [10]. As a result, we calculated several lowest eigenstates of the exciton in QW. The radiative decay rate was obtained evaluating the integral for Γ_0. In addition, the method of exterior complex scaling [14] was applied over each variable to determine the lower boundary of the continuous (essential) spectrum. It produced the complex matrix which was also used as an input for the Arnoldi algorithm.

In calculations we modeled the heavy-hole excitons in the $GaAs/Al_{0.3}Ga_{0.7}As$ heterostructures. A difference of the band gap energies of the heterostructure was taken as $\Delta E_g = 1087x + 438x^2$ meV; a ratio of barriers of QW: $V_e/V_h = 65/35$; the Luttinger parameters are following: $\gamma_1 = 6.85$, $\gamma_2 = 2.10$ for GaAs and $\gamma_1 = 3.76$, $\gamma_2 = 0.82$ for AlAs; the dielectric constant $\epsilon = 12.53$ for GaAs and $\epsilon = 10.06$ for AlAs [8, 19]. Masses and dielectric constants for ternary alloys were obtained by a linear interpolation on x.

RESULTS OF CALCULATIONS

We calculated and classified the s-like exciton states in $GaAs/Al_{0.3}Ga_{0.7}As$ QWs of various widths, L, up to 80 nm. Thus, we described the exciton spectrum as a function of QW width as a parameter. In calculations, discontinuities of the material parameters at the heterointerfaces were properly taken into account.

Figure 1 shows the energies of the s-like heavy-hole exciton states with respect to the lower boundary of the continuous spectrum, marked as a zero binding energy. The latter is defined by a sum of energies of the first quantum-confinement states of the electron and the hole in QW, $E_{e1} + E_{h1}$. So, the figure actually shows the binding energy of each state taken with a negative sign, $-E_b$. The energy levels are classified by three indices: the numbers of the electron and hole quantum-confinement states i and j; the principal number, N, of the two-dimensional Coulomb s-like ones for the in-plane relative e–h motion. Such approximate classification specifies the dominant pure state of the exciton in very narrow QW, which is contained in the calculated exciton state. This pure state is a product of three one-dimensional wave functions: for the electron in QW, for the hole in QW, and the two-dimensional Coulomb one. An increase of L leads to stronger coupling of the electron and hole in QW by the three-dimensional Coulomb potential.

The lowest curve in Fig. 1 presents the ground state of the exciton in QW, i.e. shows the exciton binding energy taken with the negative sign. The radiative decay rates, $\hbar\Gamma_0$, in μeV are written by *italic* for some curves at several values of QW widths. The upper curves are the 2s-, 3s-like exciton states of in-plane relative e–h motion as well as 1s-like states corresponding to excited quantum-confinement states. It should be noted that the Coulomb-like spectrum comprises of infinite number of bound states, which concentrate in the vicinity of the boundary $E_b = 0$ and are omitted in the figure. For $L < 20$ nm, only a set of Coulomb-like states corresponding to the ground quantum-confinement states of the electron and the hole in QW takes place. As a QW width increases, the excited exciton states drop down from the continuous spectrum and more bound states appear in the spectrum. These states are descending and ranging in the spectrum by an order of the quantum-confinement hole states. The upper Coulomb-like state for the excited quantum-confinement state is observed at $L >$ 60 nm. States with the quantum-confinement components of the same symmetry exhibit anticrossings, whereas the different symmetry lead to crossings of

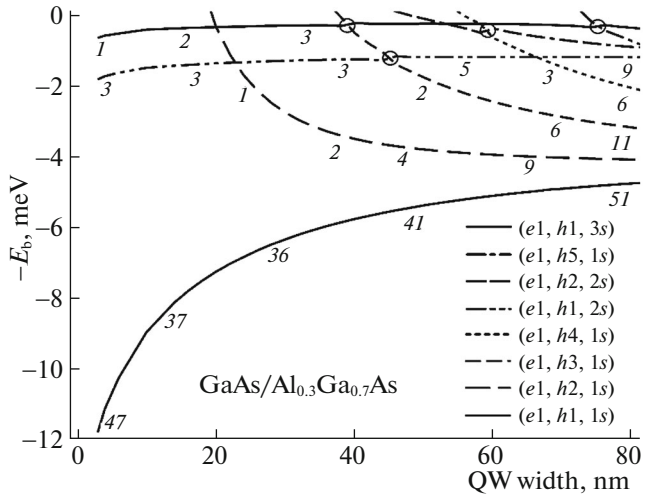

Fig. 1. The calculated energy levels of *s*-like states of the heavy-hole exciton in GaAs/Al$_{0.3}$Ga$_{0.7}$As single square QW as a function of QW width. The states are shown with respect to the lower boundary of the continuous spectrum, that is denoted by zero binding energy. The discontinuities of the material parameters are taken into account in calculations. The radiative decay rates in μeV are written by *italic*. The energy states are classified based on the types of one-dimensional functions for the factorized form of the wave function. The anticrossings of energy states of the same symmetry are shown by circles.

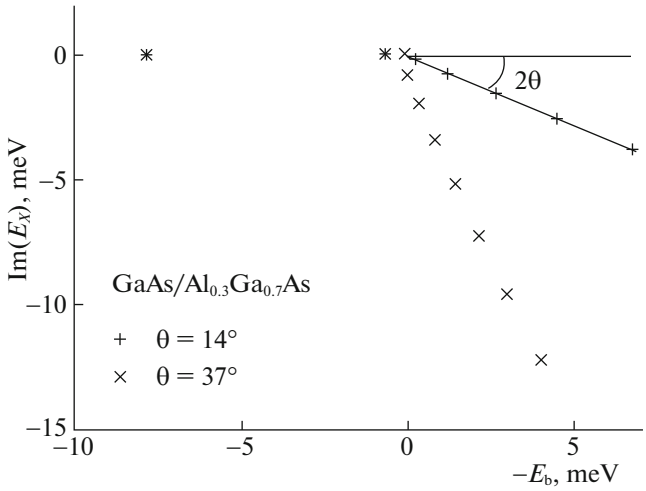

Fig. 2. The energy levels of *s*-like states of the heavy-hole exciton in GaAs/Al$_{0.3}$Ga$_{0.7}$As single square QW calculated by the complex scaling method. The width of QW equals to 10 nm. The rotated discretized continuum is clearly observed. The discontinuities of the material parameters are ignored in calculations.

states. The anticrossings are shown by circles. Numerical results are consistent with the experimental reflectance spectroscopy data for QW width of 20 nm presented in [10] as well as with data given in [20].

In order to support the statement that the sum $E_{e1} + E_{h1}$ defines the lower boundary of the continuous spectrum, we applied the exterior complex scaling method [15] to our problem. This approach allows one to study resonances in different quantum systems [14]. It introduces a complex scaling of variables in the Hamiltonian and, as a result, rotates the continuous (essential) spectrum by some angle. The bound states remain unchanged and one can distinguish them from the discretized continuum. Figure 2 shows calculated energy levels of the heavy-hole exciton states after application of the smooth rotation into the upper half-plane by angles $\theta = 14°$ and $\theta = 37°$. The QW width is $L = 10$ nm. The mismatches of material parameter were ignored in calculations. One can see the stable real energies of e–h bound states, namely the exciton energies, below the zero binding energy level, as well as the discretized continuum rotated into the lower complex half-plane. The rotation starts at the zero binding energy which corresponds to the sum $E_{e1} + E_{h1}$.

CONCLUSIONS

In summary, we calculated energies and wave functions of the *s*-like states of the heavy-hole exciton in a single square GaAs/Al$_{0.3}$Ga$_{0.7}$As QWs for QW widths up to 80 nm. The numerical solution includes the finite-difference discretization of the three-dimensional equation as well as the exact diagonalization of the obtained matrix equation. The calculated energy states were classified based on the types of one-dimensional functions for a factorized form of the wave function. The radiative decay rates of calculated states were obtained. The determined upper energy limit for states of the exciton in QW was confirmed by the complex scaling method.

ACKNOWLEDGMENTS

The work is supported by RFBR (grants nos. 16-02-00245, 18-32-00568). The calculations were carried out using the facilities of the SPbU Resource Center “Computational Center of SPbU”.

REFERENCES

1. Zh. I. Alferov, Semiconductors **32**, 1 (1998).
2. L. V. Butov, A. Imamoglu, A. V. Mintsev, et al., Phys. Rev. B **59**, 1625 (1999).
3. E. L. Ivchenko, *Optical Spectroscopy of Semiconductor Nanostructures* (Alpha Science, Harrow, 2005).
4. S. V. Poltavtsev and B. V. Stroganov, Phys. Solid State **52**, 1899 (2010).
5. S. V. Poltavtsev, Yu. P. Efimov, Yu. K. Dolgikh, et al., Solid State Commun. **199**, 47 (2014).

6. A. V. Trifonov, S. N. Korotan, A. S. Kurdyubov, et al., Phys. Rev. B **91**, 115307 (2015).
7. D. B. T. Thoai, R. Zimmermann, M. Grundmann, and D. Bimberg, Phys. Rev. B **42**, 5906(R) (1990).
8. B. Gerlach, J. Wüsthoff, M. O. Dzero, and M. A. Smondyrev, Phys. Rev. B **58**, 10568 (1998).
9. K. Sivalertporn, L. Mouchliadis, A. L. Ivanov, et al., Phys. Rev. B **85**, 045207 (2012).
10. E. S. Khramtsov, P. A. Belov, P. S. Grigoryev, et al., J. Appl. Phys. **119**, 184301 (2016).
11. P. A. Belov and E. S. Khramtsov, J. Phys.: Conf. Ser. **816**, 012018 (2017).
12. P. A. Belov, Semiconductors **52**, 551 (2018).
13. A. A. Samarskii, *The Theory of Difference Schemes* (Nauka, Moscow, 1989) [in Russian].
14. N. Moiseyev, Phys. Rep. **302**, 212 (1998).
15. C. W. McCurdy and F. Martin, J. Phys. B: At. Mol. Opt. Phys. **37**, 917 (2004).
16. P. A. Belov, V. A. Gradusov, M. V. Volkov, et al., Few-Body Syst. **58**, 114 (2017).
17. J. M. Luttinger, Phys. Rev. **102**, 1030 (1956).
18. P. A. Belov, E. R. Nugumanov, and S. L. Yakovlev, J. Phys.: Conf. Ser. **929**, 012035 (2017).
19. I. Vurgaftman, J. R. Meyer, and L. R. Ram-Mohan, J. Appl. Phys. **89**, 5815 (2001).
20. Y. Chen, N. Maharjan, Z. Liu, et al., J. Appl. Phys. **121**, 103101 (2017).